Hindawi
Journal of Nanomaterials
Volume 2019, Article ID 6821937, 9 pages
https://doi.org/10.1155/2019/6821937

Research Article

New Design of ZnO Nanorod- and Nanowire-Based NO_2 Room-Temperature Sensors Prepared by Hydrothermal Method

Vo Thanh Duoc,[1] Dang Thi Thanh Le,[1] Nguyen Duc Hoa,[1] Nguyen Van Duy,[1] Chu Manh Hung,[1] Hugo Nguyen,[2] and Nguyen Van Hieu[3,4]

[1]*International Training Institute for Materials Science (ITIMS), Hanoi University of Science and Technology (HUST), No. 1. Dai Co Viet Str., Hanoi, Vietnam*
[2]*Department of Engineering Sciences, Uppsala University, Lägerhyddsvägen 1, 751 21 Uppsala, Sweden*
[3]*Thanh Tay Institute for Advanced Study (TIAS), Phenikaa University, Yen Nghia, Ha-Dong District, Hanoi 100000, Vietnam*
[4]*Phenikaa Research and Technology Institute (PRATI), A&A Green Phoenix Group, 167 Hoang Ngan, Hanoi 100000, Vietnam*

Correspondence should be addressed to Dang Thi Thanh Le; thanhle@itims.edu.vn and Nguyen Duc Hoa; ndhoa@itims.edu.vn

Received 2 January 2019; Revised 8 March 2019; Accepted 13 March 2019; Published 9 April 2019

Academic Editor: Renyun Zhang

Room-temperature gas sensors are attracting attention because of their low power consumption, safe operation, and long-term stability. Herein, ZnO nanorods (NRs) and nanowires (NWs) were on-chip grown via a facile hydrothermal method and used for room-temperature NO_2 gas sensor applications. The ZnO NRs were obtained by a one-step hydrothermal process, whereas the NWs were obtained by a two-step hydrothermal process. To obtain ZnO NW sensor, the length of NRs was controlled short enough so that none of the nanorod-nanorod junction was made. Thereafter, the NWs were grown from the tips of no-contact NRs to form nanowire-nanowire junctions. The gas-sensing characteristics of ZnO NRs and NWs were tested against NO_2 gas at room temperature for comparison. The gas-sensing characteristics of the sensors were also tested at different applied voltages to evaluate the effect of the self-activated gas-sensing performance. Results show that the diameter of ZnO NRs and NWs is the dominant parameter of their NO_2 gas-sensing performance at room temperature. In addition, self-activation by local heating occurred for both sensors, but because the NWs were smaller and sparser than the NRs, local heating thus required a lower applied voltage with maximal response compared with the NRs.

1. Introduction

In the past decades, the rapid rise of industrialisation and urbanisation has caused severe air pollution, which primarily comes from automobile exhausts and factory emissions. This severe pollution poses a great threat to humans and all other living organisms [1]. High-performance gas sensors, particularly for the detection of toxic and explosive gases, are therefore necessary [2, 3].

Resistive gas sensors based on metal oxides, such as SnO_2 [4], NiO [5], CuO [6], WO_3 [7], and ZnO [8], are the most attractive gas sensors because of their low cost, easy operation, simple integration, and feasibility for miniaturisation [9]. Among the metal oxides, ZnO, a well-known n-type semiconductor, demonstrates the original characteristics required for an ideal gas sensor, i.e., a wide band gap (3.37 eV) and high electron mobility (210 $cm^2 \cdot V^{-1} \cdot s^{-1}$), as well as excellent chemical and thermal stability but still providing good gas-sensing performance [10–12]. Various forms of nanostructured ZnO materials, such as nanofibers, nanoparticles, nanoplates, nanorods (NRs), and nanowires (NWs), have been investigated for gas sensor applications [13–17]. One-dimensional nanostructures, such as NRs, NWs, nanotubes, and nanoneedles, were reported to possess better conductivity compared with their 2D and 3D counterparts [18] and excellent stability [19]. The gas-sensing properties of the sensors based on ZnO nanostructures are mainly dependent on the operation temperature, which controls the surface reaction kinetics and carrier mobility, resulting in the change in material conductivity [20]. In general, ZnO

gas sensors work at a relatively high temperature ranging from 300°C to 500°C [13, 14]. However, operation at high temperature may be a threat in some environments, e.g., when flammable and explosive gases are present, thereby limiting the use of the device.

Gas sensors that operate at room temperature provide not only safe operations but also low power consumption and simple fabrication, because they do not need a heating element, which is considered as the most important feature of the new-generation gas sensors [21]. The new sensors are feasible for portable, wireless, energy-saving, and cost-effective devices, in accordance with the current developing trend [9] to be applied to the internet of things [22]. Much effort was devoted to decreasing the operational temperature to as low as possible by surface modification, additive doping, preparation of hybrid/composite nanomaterials, self-heating effect [23], and light activation [21, 24]. For example, ZnO NWs were modified with Au nanograins to improve H_2S response at room temperature [25]. Navale et al. successfully decreased the working temperature of a ZnO sensor to 200°C when measuring NO_2 by using hierarchical nanostructures [26]. Lupan et al. utilised a nanofabrication process to pattern a single ZnO NR for H_2 gas detection at room temperature [27]. However, the response values were still very low, that is, the maximum response value reached only 4%. This finding can be attributed to the large diameter of the ZnO NRs used in the sensor. Cui et al. used ultraviolet (UV) illumination to trigger the gas-sensing reaction of their ZnO nanostructures to HCHO at room temperature [28]. Acharyya and Bhattacharyya [29] used ZnO nanotubes to detect alcohol at room temperature without any surface modification. Park et al. prepared a SnO_2 core/ZnO shell to measure NO_2 at room temperature with UV irradiation [30]. A remarkably enhanced response was observed under UV illumination compared with the pristine SnO_2 and ZnO NWs. UV illumination was used to increase the density of free carriers and contribute to the migration of carriers according to Comini et al. [31]. Furthermore, Costello et al. pointed out that UV illumination can promote the catalytic reaction between hydrocarbon gases and oxygen ions at room temperature [32]. In any case, the use of a noble metal catalyst and/or UV illumination to enable room-temperature sensing characteristics of ZnO leads to high fabrication and energy usage costs.

In this work, ZnO NRs and NWs were first grown on-chip by a hydrothermal method at atmospheric pressure, and their room-temperature NO_2 gas-sensing properties were studied. The gas-sensing characterisations were carried out at various applied voltages, from 1 V to 8 V, to scan through the self-activated effect. ZnO NWs have a higher response compared with ZnO NRs and require a lower applied voltage to operate. We also discussed in depth the sensing performance of sensors under the size effect and self-activation.

2. Experimental

The designs of the gas sensors based on ZnO NRs and NWs are illustrated in Figure 1. The electrodes are arranged

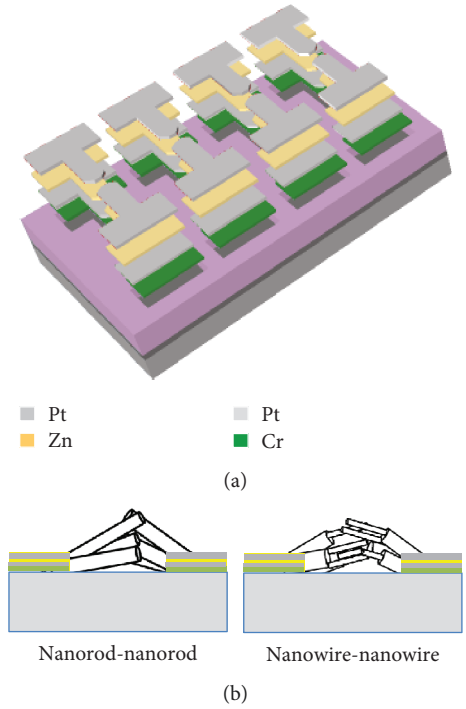

Figure 1: (a) Designs of sensor electrodes. (b) Sensors based on NR-NR (left) and NW-NW (right) junctions.

in a head-to-head configuration (Figure 1(a)). The Zn (20 nm) seed layer is sandwiched between Pt (50 nm) and Pt (20 nm)/Cr (10 nm) layers, so that the ZnO NRs can grow from the edge of the electrodes. Two types of sensors are fabricated, namely, NR-NR and NW-NW sensors (Figure 1(b)). The ZnO NRs and NWs were grown by a hydrothermal process [33, 34] using zinc nitrate hexahydrate ($Zn(NO_3)_2{\cdot}6H_2O$) and hexamethylenetetramine (HMTA) as precursors. The chemicals were of analytical grade (Sigma-Aldrich) and used without any further purification. Deionised (DI) water (>18 MΩ) obtained from a Milli-Q purifying system was used for all the solutions. The hydrothermal reaction solution for ZnO NR and NW syntheses was prepared by mixing appropriate quantities of HMTA and zinc nitrate at an equimolar ratio in a Pyrex bottle. For the fabrication of a ZnO NR sensor, a substrate with the electrode arrays facing down was immersed horizontally in the 0.02 M solution. The covered Pyrex bottle was then placed in a laboratory oven, heated to 85°C, and stored for 24 h. Subsequently, the samples were slightly rinsed three times with DI water to eliminate the residual precursors and dried under a gentle flow of nitrogen gas and in the oven at 60°C for 12 h. The fabrication of a ZnO NW sensor was similar to that of the ZnO NR sensor, but the NW synthesis was carried out using a two-step process. In the first step, solutions with a concentration of 0.0025 M were used to grow the short NRs at 85°C for 5 h. In the second step, the temperature was raised to 90°C, which was maintained for 40 h to form the secondary NWs from the tips of the short NRs. The sample was then rinsed and dried in the same way as the ZnO NR sensor. The fabricated sensors were finally annealed at 400°C for 2 h in air to stabilize the resistance before the gas-sensing

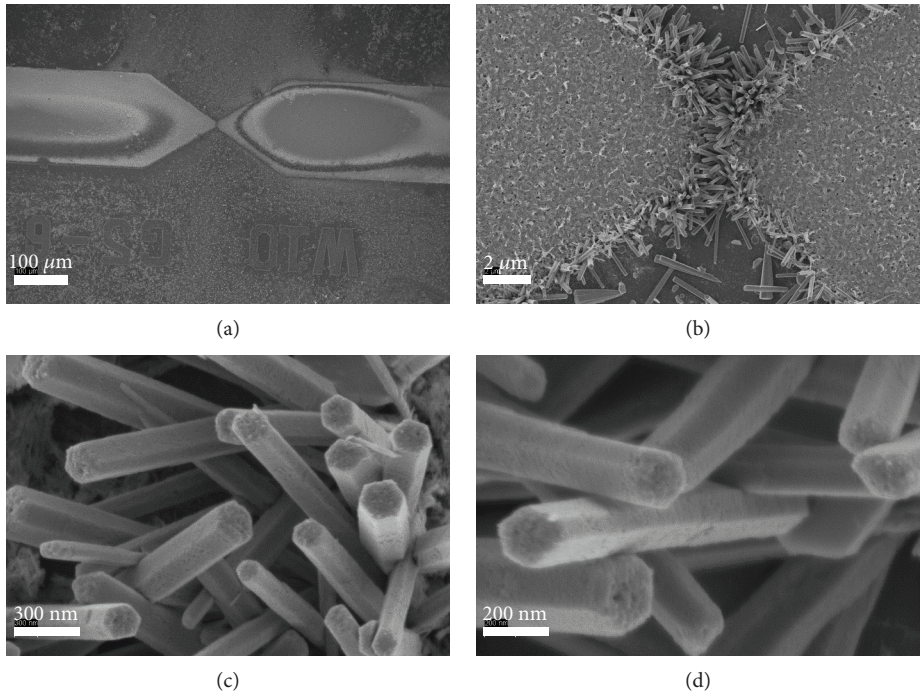

Figure 2: SEM images of the ZnO NR sensor at different magnifications: (a) head-to-head electrodes; (b) NR-NR junctions between two electrodes; (c, d) high-magnification SEM image of ZnO NRs.

measurement. The morphology, chemical composition, and structural characteristics of the synthesised ZnO NRs and NWs were investigated by scanning electron microscopy (SEM, JEOL JSM-7600F), energy-dispersive X-ray spectroscopy, high-resolution transmission electron microscopy (HRTEM, JEOL JEM-2100F), and X-ray diffraction (XRD, D8 ADVANCE). The gas-sensing properties were measured at room temperature at different applied voltages using a SourceMeter® Keithley 2602B. The measurement system was home built, as described elsewhere [35]. Dry air was used as a reference and diluting gas. During the measurements, the resistance of the sensors was continuously recorded, whereas the target gas and dry air were alternatively turned on/off. The gas response was defined as $S = R_g/R_a$ for the NO_2 oxidising gas, where R_a and R_g are the resistances of the sensor in dry air and in the target gas, respectively.

3. Results and Discussion

The morphologies of the ZnO NRs hydrothermally grown between the patterned electrodes were investigated by SEM, as shown in Figure 2. The sensor designed with head-to-head electrodes with no heater stipulates a simple fabrication process [33]. Patterning of the electrodes has been reported elsewhere, except for the deposition of a Zn seed layer of 20 nm [36]. The gap between two electrode heads is 5 μm, whereas the width is 10 μm (Figure 2(a)). As shown in Figure 2(b), the average length of ZnO NRs is about 7 μm, which is enough to bridge two electrodes. Given that the Zn seed layer is sandwiched between two Pt layers, the ZnO NRs can just start to grow from the edge of the electrode but not on the top. The tips of ZnO NRs have a clear hexagonal shape with a diameter ranging from 100 to 300 nm (Figure 2(c)). The surface of the obtained ZnO NRs is quite rough, thereby suggesting that such formation was due to the aggregation of many nuclei (Figure 2(d)). Two electrodes were connected by these ZnO NRs that formed NR-NR junctions, which acted as conducting channels for gas-sensing measurement.

The morphologies of the hydrothermally grown ZnO NWs are presented in Figure 3. In the first growth step (at a low temperature of 85°C), the ZnO NRs grew from the electrode edges. The length of the NRs was controlled by growth time, so that they did not make contact with each other (Figure 3(b)). In the second growth step (at a high temperature of 90°C), secondary NWs started to grow from the tips of the primary NRs. The average diameter and length of the NWs are approximately 20 nm and 5 μm, respectively (Figure 3(c)). The surfaces of the secondary ZnO NWs are considerably smoother than those of the NRs. Two electrodes were thereby connected by these ZnO NWs, which formed the NW-NW junctions. Gas-sensing characteristics are mainly dominated by the NW-NW junctions because of their smaller size. In addition, the cross-sectional area of NW-NW junctions is smaller than that of the NR-NR junctions; thus, some self-heating effect may be possible when testing the electrical properties under externally applied voltages. Furthermore, the junction matrix formed from these NWs is considerably sparser than that of the NRs (Figures 3(c) and 3(d)), which is expected to improve the gas-sensing performance due to the easy adsorption of gaseous molecules.

Figure 4(a) shows a low-magnification TEM image of a ZnO NR (black finger) with a diameter of approximately

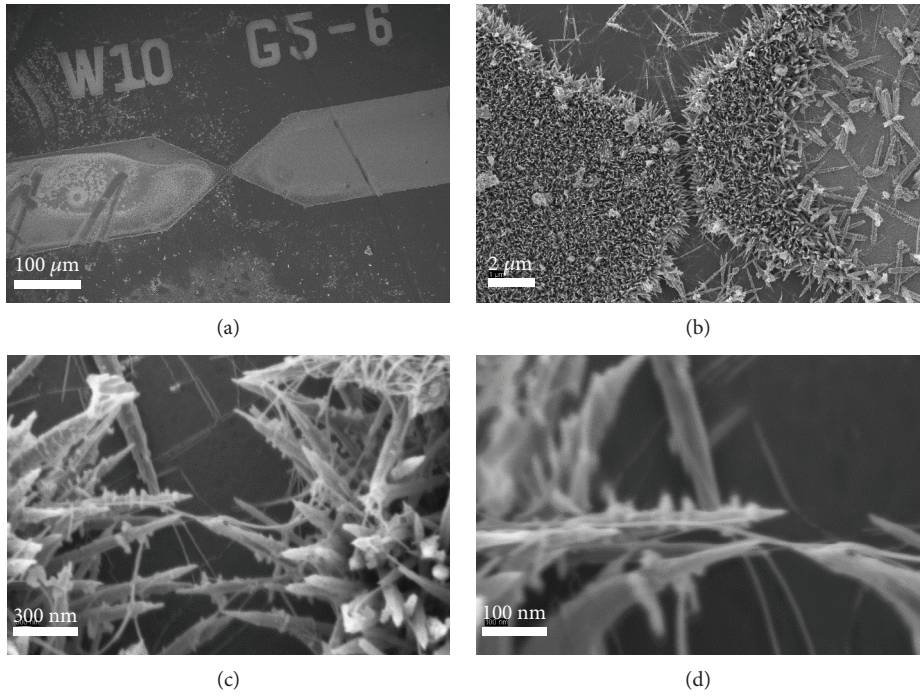

Figure 3: SEM images of the ZnO NW sensor at different magnification levels: (a) head-to-head electrodes; (b) NW-NW junctions between the head of the electrodes; (c, d) high-magnification SEM image of the NWs.

200 nm. The NR is highly crystalline with lattice fringes of 0.26 nm, corresponding to the interspace of (0002) of hexagonal ZnO, as shown in Figure 4(b). Figure 4(c) shows a TEM image of ZnO NWs with a diameter of 20-30 nm. The HRTEM image of the NWs displays lattice fringes of 0.52 nm (Figure 4(d)). No sign of any amorphous layer was observed on the surface of both NRs and NWs, thereby proving the good crystallinity of the ZnO nanostructures. The lattice fringes of the NWs are in accordance with the interspace of (0001) of hexagonal ZnO [37]. However, the surface of the NWs is not smooth due to the growth mechanism based on the aggregation of nuclei [38].

The crystal structures of the ZnO NRs and NWs were analysed by XRD. The XRD patterns of the ZnO NRs and NWs are shown in Figures 5(a) and 5(b), respectively. All the diffraction peaks of the ZnO NRs can be indexed as wurtzite ZnO (JCPDS 36-1451). Other peaks were absent, thereby demonstrating the absence of impurity or intermediate formation during the growth. Sharp and intense diffraction peaks confirmed the high degree of crystallisation of ZnO NRs. The XRD pattern of the ZnO NRs in this study differed from those of dense vertically grown NRs [39], where a strong peak centred at $2\theta = 34.64^{\circ}$ was presented. This phenomenon can be explained by the random orientation of the ZnO NRs grown from the edge of the electrodes. The XRD pattern of ZnO NWs on the other hand (Figure 4(b)) shows a very strong (002) peak at $2\theta = 34.64^{\circ}$, thereby suggesting that the preferred growth orientation is (002). This peak also exhibits a slight asymmetry, possibly due to the overlap of (002) peaks of the primary NRs.

Contact between the electrodes and the sensing materials is very important in determining their gas-sensing characteristics; therefore, the *I-V* curves of the ZnO NR and NW sensors in air were plotted, and the data are shown in Figure 6. As the bias voltage went from −15 V to 15 V, the plots were nearly linear in the gas-sensing range, i.e., 1 V to 8 V, for both sensors, thereby indicating good Ohmic contact between the sensing materials and Pt electrodes. The Schottky contact was expected to be formed at the Pt-ZnO interface, because the work function of Pt of approximately 5.93 eV was considerably higher than that of n-type ZnO of 4.66 eV [40]. Nevertheless, the linearity of the *I-V* plots proved that the Schottky contact effect was negligible, at least in the gas-sensing range. This finding was possibly due to the highly defective surface of the hydrothermally grown ZnO and/or the formation of Pt-Zn alloy at the interface during the high-temperature stabilisation annealing. Therefore, the gas-sensing characteristics are mainly based on the behaviours of ZnO NRs and NWs and their junctions.

The gas-sensing properties of the ZnO NRs and NWs in relation to different NO_2 concentrations were measured by applying various voltages at 1, 2, 4, and 8 V. The transient responses of the ZnO NRs and NWs to NO_2 at room temperature are shown in Figures 7(a) and 7(b), respectively. The plots illustrated that the resistance of the ZnO NR and NW sensors steeply increased when NO_2 gas was injected into the test chamber. The response time for the sensors to reach 90% of the saturation values was approximately 1-10 min, depending on the NO_2 concentrations and the applied voltages. Then, the resistance values dramatically turned to the previous ones when NO_2 was replaced by air in the system. The response of the sensors decreased with increasing applied voltage values. This behaviour confirmed the n-type semiconducting performance of the ZnO nanostructures.

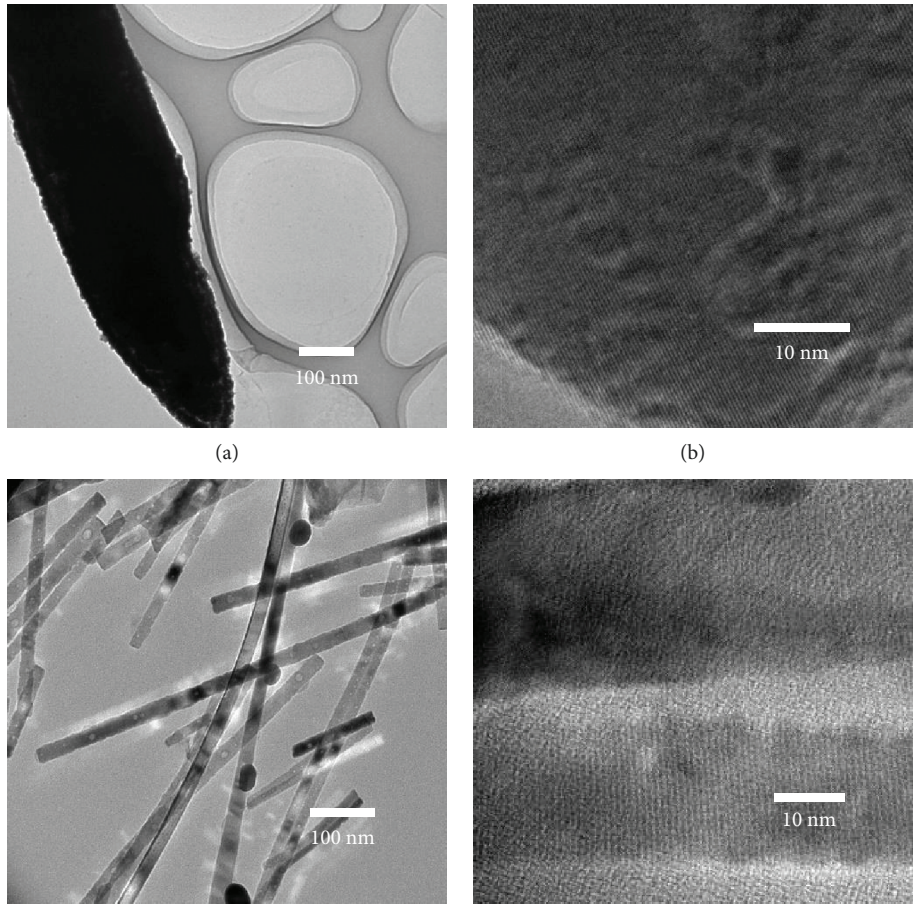

Figure 4: TEM images of ZnO (a, b) NRs and (c, d) NWs.

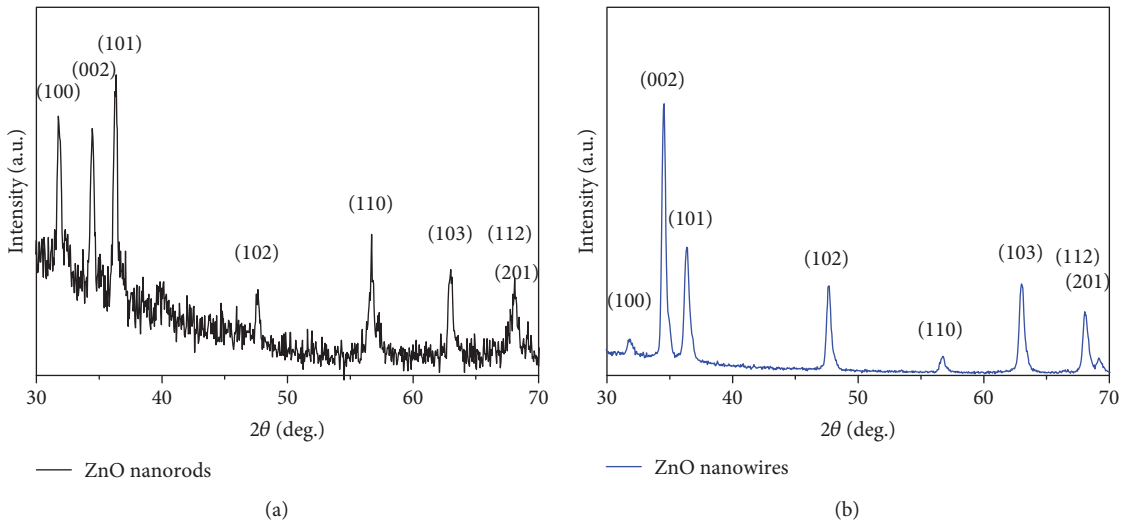

Figure 5: X-ray diffraction patterns of ZnO (a) NRs and (b) NWs.

Furthermore, the resistance values of the ZnO NW sensors were considerably higher than those of the ZnO NR sensors. This finding was attributed to the smaller diameters of the NWs compared with the NRs [33, 41]. Here, the diameter of the NWs was approximately twice the Debye length, whereas the diameter of the NRs was much larger than the Debye length. Therefore, the NW sensor showed higher sensitivity.

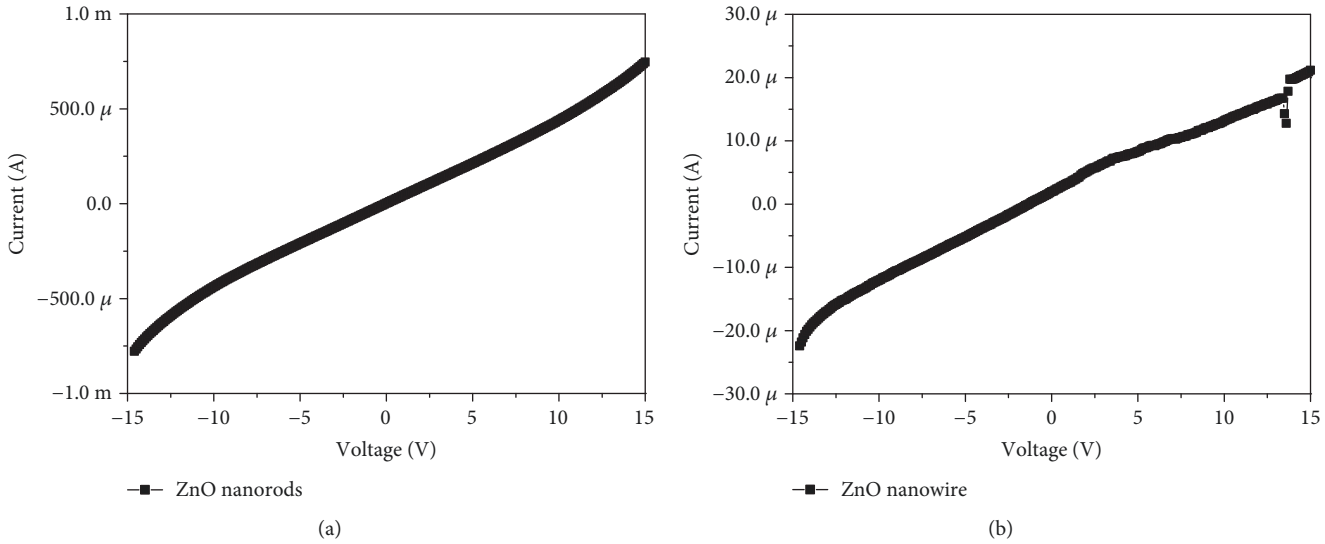

Figure 6: *I-V* characteristics of ZnO (a) NRs and (b) NWs in air.

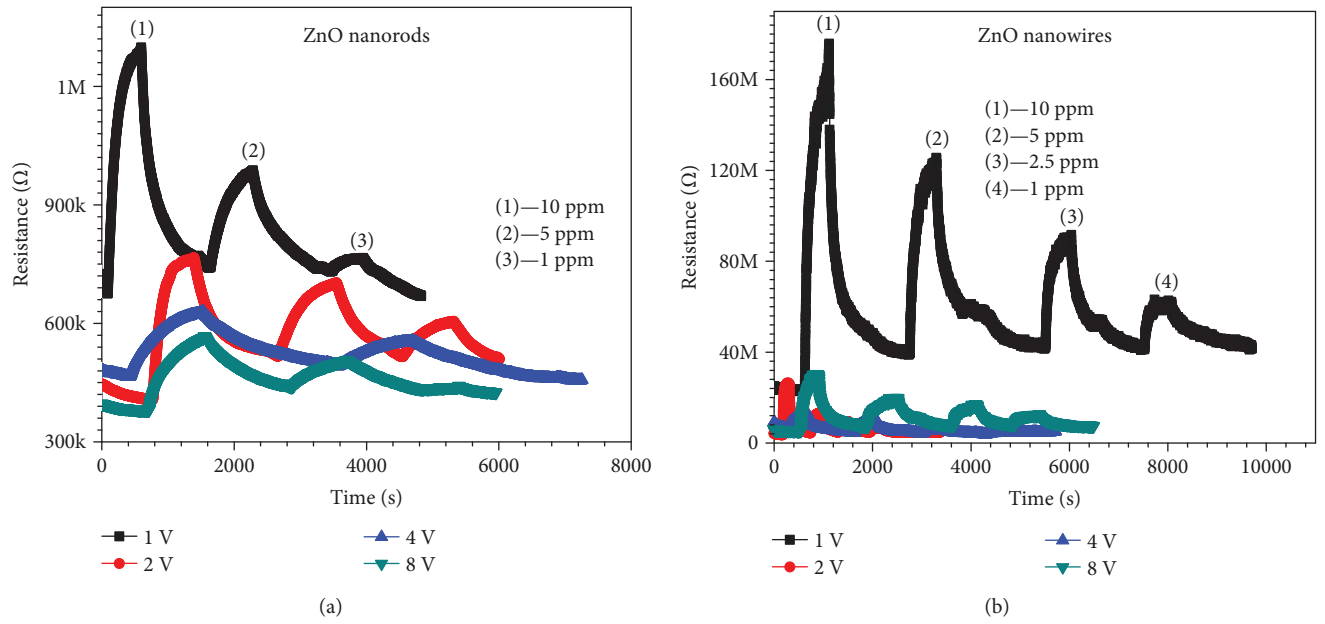

Figure 7: Transient response of (a) ZnO NRs and (b) ZnO NWs to different NO_2 concentrations at room temperature.

The response values of the ZnO NRs and NWs to NO_2 gas at room temperature under different applied voltages are calculated from the transient response plots and shown in Figure 8. The responses of both sensors at all applied voltages increased with increasing gas concentration from 1 ppm to 10 ppm. However, the NW sensor working at the applied voltage of 1 V showed the highest response, whereas the NR sensor reached the highest response at the applied voltage of 2 V. Both sensors had the lowest response values at the applied voltage of 4 V. The applied voltage affected the temperature of the sensors. By applying different voltages for gas-sensing measurement, the temperature of the sensing area can be increased differently by the self-heating effect, thereby changing the sensing performance of the sensors. Given that the density of the NWs and their diameters were considerably smaller than those of the NRs for the same applied voltage, the temperature of the NWs was expected to be higher than that of the NRs, especially at the nanojunctions [36]. Notably, the temperature-dependent sensing response of the ZnO material to NO_2 exhibited a bell shape [42] with maximum response at approximately 250°C. Therefore, the NW sensor required lower applied voltage to reach the optimal working temperature. Anyhow, this could not confirm that the temperature of the sensors under optimal applied voltages reached the value of 250°C. An attempt to measure the temperature of the NW sensor at different applied voltages by using an infrared camera (FLIR, ThermoVision A40) was made. However, because of

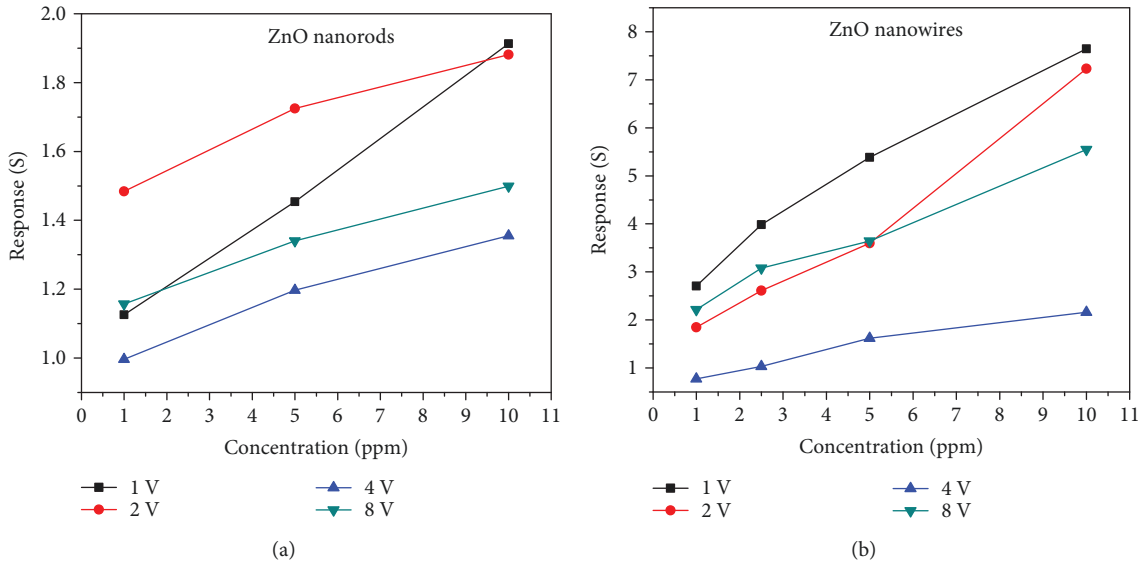

Figure 8: Response to different NO_2 concentrations of ZnO (a) NRs and (b) NWs.

Table 1: Response time/recovery time of the ZnO NR and NW sensors to various concentrations of NO_2 at different applied voltages.

Applied voltage	Nanorods			Nanowires			
	1 ppm	5 ppm	10 ppm	1 ppm	2.5 ppm	5 ppm	10 ppm
1 V	270/716	466/827	293/553	181/1153	279/834	389/1238	441/535
2 V	547/498	608/800	277/786	131/202	141/302	108/216	43/136
4 V	11/187	843/1580	762/1597	321/-	305/734	248/712	298/600
8 V	547/416	708/917	668/1008	218/572	366/491	382/745	205/498

Unit: seconds.

the limitation of camera resolution compared with the size of the NW-NW junctions and the gas-sensing area ($5 \times 10\,\mu m^2$) of the sensor, the measurement was not successful.

Table 1 summarises the response/recovery time of ZnO NR and NW sensors to different NO_2 concentrations at various applied voltages. The ZnO NW sensor exhibited shorter response times to NO_2 of 100-400 s, whereas the ZnO NR sensor showed longer response times of 200-800 s. Both sensors showed the same random tendency of recovery time. Generally, the NW sensor had its best performance in terms of response time and recovery time at an applied voltage of 2 V, whereas for the NR sensor, the best performance was achieved at an applied voltage of 1 V. It is not clear why the response and recovery time of the nanowire sensor at 2 V is the fastest. But this can be the competitive results of the nanowire-nanowire junction and the self-heating effect. At 2 V, the self-heating effect is effective enough to activate gas adsorption/desorption, but still low to make the nanowire-nanowire junction function. Anyhow, this proposed method needs further study to clarify. However, these results point out that the performance of the ZnO sensors to NO_2 is the highest by applying the appropriate voltage, thereby making this sensor very attractive for room-temperature application.

4. Conclusions

ZnO NRs and NWs were hydrothermally grown between head-to-head Pt electrodes for room-temperature NO_2 gas sensor applications. The primary ZnO NRs were grown by a one-step hydrothermal process, whereas the secondary NWs were grown via a two-step process. The diameter of the ZnO NWs was considerably smaller than that of the ZnO NRs at 20-30 nm compared with 100-300 nm. The NW sensors showed much higher response to NO_2 than the NR sensors at room temperature, and such a response occurred at the applied voltage of 1 and 2 V for the respective sensors. The NWs with a small diameter provided not only a large effective surface area and Debye length compatible to the depletion layer but also a higher temperature by the self-heated effect, thereby leading to a lower supplied voltage with maximal sensing performance.

Data Availability

The data used to support the findings of this study are included within the article.

Conflicts of Interest

The authors declare no conflict of interests regarding the publication of this paper.

Acknowledgments

This work was supported by the Vietnam National Foundation for Science and Technology Development (NAFOSTED) under grant number 103.02-2015.43.

References

[1] T. H. Le, T. N. Thanh Nguyen, K. Lasko, S. Ilavajhala, K. P. Vadrevu, and C. Justice, "Vegetation fires and air pollution in Vietnam," *Environmental Pollution*, vol. 195, pp. 267–275, 2014.

[2] J. Hu, J. Yang, W. Wang et al., "Synthesis and gas sensing properties of NiO/SnO_2 hierarchical structures toward ppb-level acetone detection," *Materials Research Bulletin*, vol. 102, pp. 294–303, 2018.

[3] D. N. Oosthuizen, D. E. Motaung, and H. C. Swart, "Selective detection of CO at room temperature with CuO nanoplatelets sensor for indoor air quality monitoring manifested by crystallinity," *Applied Surface Science*, vol. 466, pp. 545–553, 2019.

[4] L. V. Thong, N. D. Hoa, D. T. T. le et al., "On-chip fabrication of SnO_2-nanowire gas sensor: the effect of growth time on sensor performance," *Sensors and Actuators B: Chemical*, vol. 146, no. 1, pp. 361–367, 2010.

[5] M. Tonezzer, T. T. L. Dang, Q. H. Tran, and S. Iannotta, "Dual-selective hydrogen and ethanol sensor for steam reforming systems," *Sensors and Actuators B: Chemical*, vol. 236, pp. 1011–1019, 2016.

[6] L. D. Duc, D. T. T. le, N. V. Duy, N. D. Hoa, and N. V. Hieu, "Single crystal cupric oxide nanowires: length- and density-controlled growth and gas-sensing characteristics," *Physica E: Low-dimensional Systems and Nanostructures*, vol. 58, pp. 16–23, 2014.

[7] P. Van Tong, N. D. Hoa, V. Van Quang, N. Van Duy, and N. Van Hieu, "Diameter controlled synthesis of tungsten oxide nanorod bundles for highly sensitive NO_2 gas sensors," *Sensors and Actuators B: Chemical*, vol. 183, pp. 372–380, 2013.

[8] T. Van Dang, N. D. Hoa, N. Van Duy, and N. Van Hieu, "Chlorine gas sensing performance of on-chip grown ZnO, WO_3, and SnO_2 nanowire sensors," *ACS Applied Materials & Interfaces*, vol. 8, no. 7, pp. 4828–4837, 2016.

[9] K. Nguyen, C. M. Hung, T. M. Ngoc et al., "Low-temperature prototype hydrogen sensors using Pd-decorated SnO_2 nanowires for exhaled breath applications," *Sensors and Actuators B: Chemical*, vol. 253, pp. 156–163, 2017.

[10] H. Nguyen, C. T. Quy, N. D. Hoa et al., "Controllable growth of ZnO nanowires grown on discrete islands of Au catalyst for realization of planar-type micro gas sensors," *Sensors and Actuators B: Chemical*, vol. 193, pp. 888–894, 2014.

[11] Q. Zhou, B. Xie, L. Jin, W. Chen, and J. Li, "Hydrothermal synthesis and responsive characteristics of hierarchical zinc oxide nanoflowers to sulfur dioxide," *Journal of Nanotechnology*, vol. 2016, Article ID 6742104, 6 pages, 2016.

[12] Z. Q. Zheng, J. D. Yao, B. Wang, and G. W. Yang, "Light-controlling, flexible and transparent ethanol gas sensor based on ZnO nanoparticles for wearable devices," *Scientific Reports*, vol. 5, no. 1, article 11070, 2015.

[13] Z. L. Wang, "Zinc oxide nanostructures: growth, properties and applications," *Journal of Physics: Condensed Matter*, vol. 16, no. 25, pp. R829–R858, 2004.

[14] J.-H. Lee, J.-Y. Kim, A. Mirzaei, H. Kim, and S. Kim, "Significant enhancement of hydrogen-sensing properties of ZnO nanofibers through NiO loading," *Nanomaterials*, vol. 8, no. 11, p. 902, 2018.

[15] Q. Ma, Y. Fang, Y. Liu et al., "Facile synthesis of ZnO morphological evolution with tunable growth habits: achieving superior gas-sensing properties of hemispherical ZnO/Au heterostructures for triethylamine," *Physica E: Low-dimensional Systems and Nanostructures*, vol. 106, pp. 180–186, 2019.

[16] M. Tonezzer and S. Iannotta, "H_2 sensing properties of two-dimensional zinc oxide nanostructures," *Talanta*, vol. 122, pp. 201–208, 2014.

[17] N. D. Hoa, N. V. Duy, S. A. el-Safty, and N. V. Hieu, "Meso-/nanoporous semiconducting metal oxides for gas sensor applications," *Journal of Nanomaterials*, vol. 2015, Article ID 972025, 14 pages, 2015.

[18] A. Kolmakov and M. Moskovits, "Chemical sensing and catalysis by one-dimensional metal-oxide nanostructures," *Annual Review of Materials Research*, vol. 34, no. 1, pp. 151–180, 2004.

[19] V. V. Sysoev, T. Schneider, J. Goschnick et al., "Percolating SnO_2 nanowire network as a stable gas sensor: direct comparison of long-term performance *versus* SnO_2 nanoparticle films," *Sensors and Actuators B: Chemical*, vol. 139, no. 2, pp. 699–703, 2009.

[20] N. T. Phuong Nhung, P. Van Tong, C. M. Hung et al., "Nanoporous ZnO nanostructure synthesis by a facile method for superior sensitivity ethanol sensor applications," *RSC Advances*, vol. 6, no. 69, pp. 64215–64218, 2016.

[21] L. Zhu and W. Zeng, "Room-temperature gas sensing of ZnO-based gas sensor: a review," *Sensors and Actuators A: Physical*, vol. 267, pp. 242–261, 2017.

[22] M. Cerchecci, F. Luti, A. Mecocci, S. Parrino, G. Peruzzi, and A. Pozzebon, "A low power IoT sensor node architecture for waste management within smart cities context," *Sensors*, vol. 18, no. 4, article 1282, 2018.

[23] H. M. Tan, C. Manh Hung, T. M. Ngoc et al., "Novel self-heated gas sensors using on-chip networked nanowires with ultralow power consumption," *ACS Applied Materials & Interfaces*, vol. 9, no. 7, pp. 6153–6162, 2017.

[24] J. Zhang, X. Liu, G. Neri, and N. Pinna, "Nanostructured materials for room-temperature gas sensors," *Advanced Materials*, vol. 28, no. 5, pp. 795–831, 2016.

[25] N. S. Ramgir, P. K. Sharma, N. Datta et al., "Room temperature H_2S sensor based on Au modified ZnO nanowires," *Sensors and Actuators B: Chemical*, vol. 186, pp. 718–726, 2013.

[26] Y. H. Navale, S. T. Navale, N. S. Ramgir et al., "Zinc oxide hierarchical nanostructures as potential NO_2 sensors," *Sensors and Actuators B: Chemical*, vol. 251, pp. 551–563, 2017.

[27] O. Lupan, G. Chai, and L. Chow, "Novel hydrogen gas sensor based on single ZnO nanorod," *Microelectronic Engineering*, vol. 85, no. 11, pp. 2220–2225, 2008.

[28] J. Cui, L. Shi, T. Xie, D. Wang, and Y. Lin, "UV-light illumination room temperature HCHO gas-sensing mechanism of ZnO with different nanostructures," *Sensors and Actuators B: Chemical*, vol. 227, pp. 220–226, 2016.

[29] D. Acharyya and P. Bhattacharyya, "Alcohol sensing performance of ZnO hexagonal nanotubes at low temperatures: a

qualitative understanding," *Sensors and Actuators B: Chemical*, vol. 228, pp. 373–386, 2016.

[30] S. Park, S. An, Y. Mun, and C. Lee, "UV-enhanced NO_2 gas sensing properties of SnO_2-core/ZnO-shell nanowires at room temperature," *ACS Applied Materials & Interfaces*, vol. 5, no. 10, pp. 4285–4292, 2013.

[31] E. Comini, A. Cristalli, G. Faglia, and G. Sberveglieri, "Light enhanced gas sensing properties of indium oxide and tin dioxide sensors," *Sensors and Actuators B: Chemical*, vol. 65, no. 1-3, pp. 260–263, 2000.

[32] B. P. J. de Lacy Costello, R. J. Ewen, N. M. Ratcliffe, and M. Richards, "Highly sensitive room temperature sensors based on the UV-LED activation of zinc oxide nanoparticles," *Sensors and Actuators B: Chemical*, vol. 134, no. 2, pp. 945–952, 2008.

[33] M. Jiao, N. Van Duy, D. D. Trung et al., "Comparison of NO_2 gas-sensing properties of three different ZnO nanostructures synthesized by on-chip low-temperature hydrothermal growth," *Journal of Electronic Materials*, vol. 47, no. 1, pp. 785–793, 2018.

[34] L. Vayssieres, "Growth of arrayed nanorods and nanowires of ZnO from aqueous solutions," *Advanced Materials*, vol. 15, no. 5, pp. 464–466, 2003.

[35] M. Tonezzer, D. T. T. Le, S. Iannotta, and N. Van Hieu, "Selective discrimination of hazardous gases using one single metal oxide resistive sensor," *Sensors and Actuators B: Chemical*, vol. 277, pp. 121–128, 2018.

[36] T. M. Ngoc, N. van Duy, C. M. Hung et al., "Ultralow power consumption gas sensor based on a self-heated nanojunction of SnO_2 nanowires," *RSC Advances*, vol. 8, no. 63, pp. 36323–36330, 2018.

[37] H. V. Han, N. D. Hoa, P. V. Tong, H. Nguyen, and N. V. Hieu, "Single-crystal zinc oxide nanorods with nanovoids as highly sensitive NO_2 nanosensors," *Materials Letters*, vol. 94, pp. 41–43, 2013.

[38] V. Strano, R. G. Urso, M. Scuderi et al., "Double role of HMTA in ZnO nanorods grown by chemical bath deposition," *Journal of Physical Chemistry C*, vol. 118, no. 48, pp. 28189–28195, 2014.

[39] N. Van Quy, V. A. Minh, N. Van Luan, V. N. Hung, and N. Van Hieu, "Gas sensing properties at room temperature of a quartz crystal microbalance coated with ZnO nanorods," *Sensors and Actuators B: Chemical*, vol. 153, no. 1, pp. 188–193, 2011.

[40] F. Yan, Y. Wang, J. Zhang, Z. Lin, J. Zheng, and F. Huang, "Schottky or Ohmic metal-semiconductor contact: influence on photocatalytic efficiency of ag/ZnO and Pt/ZnO model systems," *ChemSusChem*, vol. 7, no. 1, pp. 101–104, 2014.

[41] C. T. Quy, N. X. Thai, N. D. Hoa et al., "C_2H_5OH and NO_2 sensing properties of ZnO nanostructures: correlation between crystal size, defect level and sensing performance," *RSC Advances*, vol. 8, no. 10, pp. 5629–5639, 2018.

[42] F.-T. Liu, S.-F. Gao, S.-K. Pei, S.-C. Tseng, and C.-H. J. Liu, "ZnO nanorod gas sensor for NO_2 detection," *Journal of the Taiwan Institute of Chemical Engineers*, vol. 40, no. 5, pp. 528–532, 2009.